Muon Spin Relaxation Studies of Magnetic Order in $Y_{1-x}U_xPd_3$ and UPd_4

W. D. Wu, A. Keren, L. P. Le, G. M. Luke, B. J. Sternlieb,* and Y. J. Uemura
Department of Physics, Columbia University, New York, New York 10027

C. L. Seaman, Y. Dalichaouch, and M. B. Maple
Department of Physics and Institute of Pure and Applied Physical Sciences, University of California, San Diego, La Jolla, California 92093
(Received 22 July 1993)

We have performed muon spin relaxation (μSR) measurements of polycrystalline specimens of $Y_{1-x}U_xPd_3$ with $x=0.1$, 0.2, 0.4 and UPd_4. We demonstrate that UPd_4 and $Y_{0.6}U_{0.4}Pd_3$ exhibit spin glass order, while the predominant volume fraction remains nonmagnetic at $T\to 0$ in $Y_{0.8}U_{0.2}Pd_3$ and the muon spin relaxation rate becomes even smaller in $Y_{0.9}U_{0.1}Pd_3$, indicating the disappearance of magnetic order with decreasing U concentration x. These results are discussed in terms of the competition between the crystalline electric field splitting Δ_{CEF} and the exchange coupling J.

PACS numbers: 76.75.+i, 75.10.Nr, 75.30.Mb

Rare earth and actinide alloys have demonstrated interesting magnetism due to the combination of the Kondo effect [1,2], RKKY exchange interaction [2], and crystalline electric field (hereafter CEF) splitting [3]. The Kondo effect can manifest itself in various forms, including that of the so-called coherent Kondo lattice, thought to be responsible for heavy fermion behavior [4]. Recently, Cox proposed the possibility of a two-channel quadrupolar Kondo effect, based on a nonmagnetic Γ_3 ground state doublet, to explain the lack of strong magnetic field dependence in the specific heat and susceptibility of UBe_{13} [5]. An investigation of the $Y_{1-x}U_xPd_3$ alloy system by Seaman *et al.* revealed that the electrical resistivity $\rho(T)$, electronic specific heat $\Delta C(T)$, and entropy $S(T)-S(0)$ for $x\leq 0.2$ exhibited non-Fermi-liquid behavior, apparently due to a two-channel quadrupolar Kondo effect [6]. Magnetic susceptibility measurements on $Y_{1-x}U_xPd_3$ with U concentrations $0.3\leq x\leq 0.5$ show spin-glass-like behavior [7], but no direct confirmation of magnetic order exists.

In this paper, we report zero field (ZF) and longitudinal field (LF) μSR measurements on $Y_{1-x}U_xPd_3$ and the related compound UPd_4 [8]. We found that UPd_4 and $Y_{0.6}U_{0.4}Pd_3$ exhibit spin glass order, while the predominant volume fraction remains nonmagnetic at $T\to 0$ in $Y_{0.8}U_{0.2}Pd_3$ and the muon spin relaxation rate becomes even smaller in $Y_{0.9}U_{0.1}Pd_3$. These results demonstrate disappearance of magnetic order with decreasing U concentration x. We show that this behavior can be understood in terms of the competition between Δ_{CEF} (the energy separation between the CEF ground state and the first excited state) and J (the exchange interaction coupling between U^{4+} ions).

Polycrystalline specimens of $Y_{1-x}U_xPd_3$ with $x=0.1$, 0.2, 0.4 and UPd_4 were prepared at UCSD by arc melting in an argon atmosphere. Powder x-ray diffraction indicated the cubic Cu_3Au-type structure for $0\leq x\leq 0.5$. UPd_4 has the same cubic structure with stoichiometry $\circ_{0.25}U_{0.75}Pd_3$, where $\circ$ represents a vacancy [6,7]. Our μSR measurements were performed at the TRIUMF M15 and M20 muon channels. ZF-μSR [9] is very sensitive to static magnetic order. The μSR relaxation function $G(t)$ due to static random fields, such as nuclear dipolar fields [10] or random fields in spin glass systems [11], is characterized by a recovery to $\frac{1}{3}$ following depolarization. The dynamic fluctuation of fields also causes muon spin relaxation, but without the $\frac{1}{3}$ recovery. Static and dynamic fields can be further distinguished through the application of longitudinal magnetic fields (LF-μSR).

Figures 1(a)–1(d) show the ZF-μSR time spectra $A(t)/A(0)$ obtained from the muon decay asymmetry $A(t)$ observed in $Y_{1-x}U_xPd_3$ and UPd_4. Nuclear dipolar fields in the specimens are negligible; the calculated width is $\Delta\leq 0.03\ \mu s^{-1}$. A roughly 10% Gaussian background signal, corresponding to muons stopping in the cryostat walls, has been subtracted from the total asymmetry for each sample. At the lowest temperature, $A(t)/A(0)$ in UPd_4 and $Y_{0.6}U_{0.4}Pd_3$ recovers to $\sim\frac{1}{3}$ following the initial depolarization, clearly indicating spin glass order. Weak magnetism appears below $T\sim 1$ K in $Y_{0.8}U_{0.2}Pd_3$ and is essentially absent in $Y_{0.9}U_{0.1}Pd_3$.

In a concentrated spin glass, the random local fields at the muon sites can be represented by a Gaussian distribution $P_G(H,\Delta)=(\gamma_\mu/\sqrt{2\pi}\Delta)\exp(-\gamma_\mu^2H^2/2\Delta^2)$ with a width Δ/γ_μ. In the model of coexisting static and dynamic random fields, the muon spin relaxation function $G_G(Q,\Delta,\nu,t)$ is given by $G_G(Q,\Delta,\nu,t)=G_1(t)G_2(t)$ with

$$G_1(t)=\tfrac{1}{3}+\tfrac{2}{3}(1-Q\Delta^2t^2)\exp(-\tfrac{1}{2}Q\Delta^2t^2)\,, \quad (1)$$

$$G_2(t)=\exp[-2(1-Q)\Delta^2t/\nu]\,, \quad (2)$$

where $G_1(t)$ is the static Kubo-Toyabe function [10] for a finite order parameter Q [$G_1(t)=1$ for $Q=0$], while $G_2(t)$ represents the effect of dynamic fluctuations with the fluctuation rate $\nu\gg\Delta$.

In a dilute alloy spin glass, in contrast, different muon sites have different variable ranges of random local fields when spin fluctuations occur: A muon site closer to a

0031-9007/94/72(23)/3722(4)$06.00

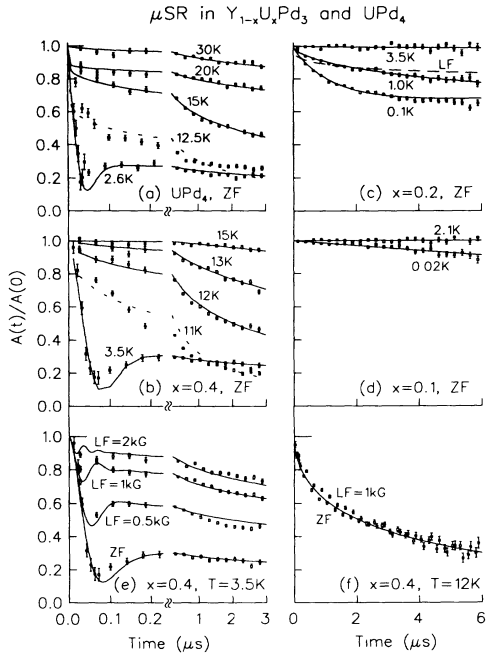

FIG. 1. The μSR time spectra $A(t)/A(0)$ observed in zero external field in (a) UPd_4, (b) $Y_{0.6}U_{0.4}Pd_3$, (c) $Y_{0.8}U_{0.2}Pd_3$, and (d) $Y_{0.9}U_{0.1}Pd_3$. In (a) and (b), the solid lines are best fits and the dashed lines represent the fits with the dynamic relaxation rate λ_d fixed to be the values obtained from longitudinal field measurements. The dashed line in (c) indicates $A(t)/A(0)$ measured at $T=0.1$ K and LF=100 G. (e) and (f) show $A(t)/A(0)$ observed in $Y_{0.6}U_{0.4}Pd_3$ in longitudinal external fields at $T=3.5$ and 12 K, respectively.

magnetic moment has a larger width Δ/γ_μ. Taking this into account, Uemura *et al.* [11] calculated the relaxation function $G(a_s,\lambda_d,t)$ in dilute alloy spin glasses by using a probability function $\rho(\Delta,a)$, which describes the probability of finding a muon site with the field width Δ/γ_μ. $G(a_s,\lambda_d,t)$ was then given as $G(a_s,\lambda_d,t)=\int_0^\infty G_G(Q,\Delta,\nu,t)\rho(\Delta,a)d\Delta$, while the total Lorentzian distribution of the local field, with the width a/γ_μ, is recovered as $P_L(H,a)=\int_0^\infty P_G(H,\Delta)\rho(\Delta,a)d\Delta$.

The $Y_{1-x}U_xPd_3$ system lies between these two limiting cases: dense moments and dilute moments. The muon spin relaxation function can be obtained by assuming a modified probability function $\rho(\Delta,a)$ [12]. However, for simplicity, we adopt the follwing phenomenological relaxation function $G(a_s,\alpha,\lambda_d,\beta,t)$:

$$G(a_s,\alpha,\lambda_d,\beta,t)=\{\tfrac{1}{3}+\tfrac{2}{3}[1-(a_st)^\alpha]\exp[-(a_st)^\alpha/\alpha]\}\times\exp[-(\lambda_dt)^\beta], \quad (3)$$

where a_s represents the width of the static random field in units of μs^{-1} and λ_d is the dynamic relaxation rate. This relaxation function interpolates the two limiting cases of Gaussian [with $\alpha=2$ and $\beta=1$, leading to $G_G(Q,\Delta,\nu,t)$] and Lorentzian [with $\alpha=1$ and $\beta=\frac{1}{2}$, leading to the limiting case of small λ_d given by Eq. (24) in Ref. [11]] field distributions. This phenomenological line shape can be reproduced by using microscopic arguments [12].

The ZF asymmetry measured in $Y_{0.6}U_{0.4}Pd_3$ was fitted with $A_0G(a_s,\alpha,\lambda_d,\beta,t)$ in the time region $0\le t\le 8$ μs. The ZF asymmetry in UPd_4 was fitted with $A_0G(a_s,\alpha,\lambda_d,\beta,t)+A_m\epsilon(t)$, where $A_0G(a_s,\alpha,\lambda,\beta,t)$ is due to the spin glass order in a large volume fraction $[A_0/(A_0+A_m)\approx 0.9]$ and the step function $\epsilon(t)$ [$\epsilon(0)=1$ and $\epsilon(t)=0$ for $t>0$] represents an initial asymmetry drop due to magnetic order below $\sim$30 K (also apparent in magnetization measurements [13]) in a small volume fraction ($\sim$10%). In Figs. 1(a) and 1(b), the solid lines are best fits [14] and the dashed lines represent fits with the dynamic relaxation rate λ_d fixed to the values obtained from longitudinal field measurements. The parameter $\alpha\approx 1.6$ obtained at the lowest temperatures for both $Y_{0.6}U_{0.4}Pd_3$ and UPd_4 indicates a field distribution between Gaussian and Lorentzian.

We fitted the ZF asymmetry in $Y_{0.8}U_{0.2}Pd_3$ and $Y_{0.9}U_{0.1}Pd_3$ to the sum $A_0G(a_s,\alpha,\lambda_d,\beta,t)+A_n$, where $A_n/(A_0+A_n)$ represents the nonmagnetic volume fraction, and α and β are fixed to 1 and $\frac{1}{2}$, respectively, due to the rather dilute magnetic moments. For $x=0.2$, the nonmagnetic volume fraction $A_n/(A_0+A_n)$ can be unambiguously determined to be $\sim(61\pm 5)$%, based on the saturation of $A(t)/A(0)$ at $\sim$0.7 observed at $T=0.1$ K, as shown in Fig. 1(c). For this specimen, the dynamic relaxation rate λ_d is fixed to values obtained by fitting the LF-μSR time spectra (LF=100 G) to $A_n+A_0\times\exp(-\sqrt{\lambda t})$. The observed time spectrum $A(t)/A(0)$ in a longitudinal field LF=100 G [the dashed line in Fig. 1(c)] indicates that the local magnetic fields in the magnetic volume are predominantly static at $T=0.1$ K.

As shown in Fig. 1(d), the relaxation rate observed in the $x=0.1$ system is much smaller than that in the $x=0.2$ system, suggesting that the tendency towards magnetic order rapidly weakens as the U concentration x is decreased. When the relaxation rate is very small, $A(t)/A(0)$ does not reach its minimum (or saturating) value in the time region of μSR measurements (0–8 μs). As a result, we cannot distinguish the case where the full volume is magnetic with very small magnetic moments ($A_n=0$ with very small a_s) from the other case where a partial volume fraction is magnetic with less small magnetic moments ($A_n\neq 0$ with somewhat larger a_s). Therefore, the nonmagnetic volume fraction $A_n/(A_0+A_n)$ cannot be unambiguously determined for $x=0.1$. However, the upper limit of the static random field $(a_s)_{\max}\approx 0.1$ μs^{-1} in the magnetic region can be obtained for the largest possible value of $A_n/(A_0+A_n)\approx 90$%. If $A_n/(A_0+A_n)$ is smaller than 90%, a smaller value of a_s is required to fit the data. At this U concentration, a longitudinal field LF=100 G completely decouples the μSR spectra ($\lambda_d=0$), indicating that the observed small relaxation is caused mainly by static fields.

Figure 2(a) shows the temperature dependence of the width of the static random field a_s in $Y_{0.6}U_{0.4}Pd_3$, and in

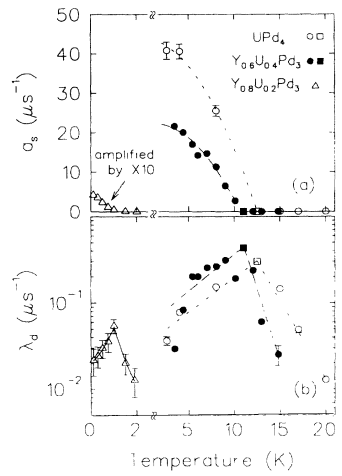

FIG. 2. (a) Temperature dependence of the static random field a_s in $Y_{0.6}U_{0.4}Pd_3$, in the region of spin glass order in UPd_4, and in the magnetic region of $Y_{0.8}U_{0.2}Pd_3$. The onset of spin glass order is seen at $T_g = 12.5 \pm 1$ K for UPd_4, at 11.0 ± 0.5 K for $Y_{0.6}U_{0.4}Pd_3$, and at 1.0 ± 0.5 K for $Y_{0.8}U_{0.2}Pd_3$ within the magnetic partial volume, respectively. (b) Temperature dependence of the dynamic relaxation rate λ_d in $Y_{0.6}U_{0.4}Pd_3$ and UPd_4 and $Y_{0.8}U_{0.2}Pd_3$. In both (a) and (b), the closed and open squares as well as triangles represent the results of fitting with the dynamic relaxation rate λ_d fixed to be the values obtained from longitudinal field measurements. All lines are guides to the eye.

the region of spin glass order in UPd_4. The onset of spin glass order is seen at $T_g = 12.5 \pm 1$ K in UPd_4 and at 11.0 ± 0.5 K in $Y_{0.6}U_{0.4}Pd_3$, with $a_s = 40.8$ and 21.7 μs^{-1}, respectively, as $T \to 0$. For $Y_{0.8}U_{0.2}Pd_3$, we plot the width of the static random field a_s in the magnetic

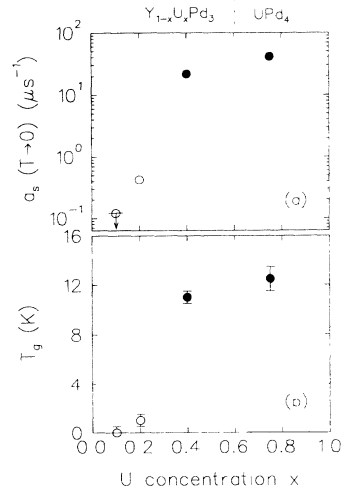

FIG. 3. (a) Low temperature width of the static random field $a_s(T \to 0)$ as a function of uranium concentration x. (b) Magnetic phase diagram of the $Y_{1-x}U_xPd_3$ and UPd_4 systems. Open circles in (a) and (b) represent the values in the magnetic volume fraction of the specimens. The arrow in (a) representing a_s in $Y_{0.9}U_{0.1}Pd_3$ in the magnetic region is smaller than 0.1 μs^{-1} if the nonmagnetic volume fraction is less than 90%.

fraction (40% volume), which indicates the freezing temperature $T_g = 1.0 \pm 0.5$ K within the magnetic partial volume.

The static width parameter a_s approximately represents the half width at half maximum (HWHM) W of the field distribution ($a_s/\gamma_\mu = 1.0W$ for Lorentzian and $0.85W$ for Gaussian distribution). We can compare the observed values of a_s with a computer simulation of W for dipolar fields from the U moments, assuming a muon site. Unfortunately, the site location is not known accurately. If we choose a likely candidate site at the center of the cubic primitive cell formed by eight Y^{3+} or U^{4+} ions, then the observed values of a_s correspond to about $\mu \sim 1 \mu_B$ U moment in both $Y_{1-x}U_xPd_3$ and UPd_4. This crude estimate is consistent with a neutron scattering result $\mu = 0.8\mu_B$ obtained in UPd_4 [15]. We note that the reduction of the U moment from the free ion value $gJ\mu_B = 3.2\mu_B$ demonstrates the influence of the CEF.

The LF-μSR time spectra in $Y_{0.6}U_{0.4}Pd_3$ are shown in Figs. 1(e)-1(f). Clear decoupling at $T = 3.5$ K indicates nearly static magnetic order. The measured asymmetry is well described by the calculated relaxation function

$$G(a_s,\alpha,\lambda_d,\beta,H,t) = \exp[-(\lambda_d t)^\beta] \times \int_0^\infty G_1(\Delta,H,t)\rho(\Delta,a_s)d\Delta$$

using values of a_s, λ_d, and β from the ZF measurements and a corresponding probability function $\rho(\Delta,a_s)$ for $\alpha = 1.6$, as shown by solid lines in Fig. 1(e). The absence of decoupling at $T = 12.0$ K shown in Fig. 1(f) indicates fluctuation of the U^{4+} moments with the static random field $a_s = 0$, consistent with $T_g \approx 11.0$ K obtained in the ZF measurements. The LF-μSR spectra measured in UPd_4 show the same behavior as those of $Y_{0.6}U_{0.4}Pd_3$.

Figure 2(b) shows the temperature dependence of the dynamic relaxation rate λ_d in $Y_{0.6}U_{0.4}Pd_3$ and UPd_4 and $Y_{0.8}U_{0.2}Pd_3$ (within the magnetic volume). The rapid increase of λ_d as T is decreased towards T_g indicates the critical slowing down of the spin fluctuations [11]. For all the three samples plotted in Fig. 2, the peak temperature of λ_d corresponds well with the temperature below which a_s becomes nonzero, providing reliable values for the freezing temperature T_g.

Figure 3(a) shows the width of the static random field a_s at the lowest measured temperature as a function of U concentration x. We plot the width in the magnetic volume (40%) for $x = 0.2$, while the upper limit value $(a_s)_{max}$ is plotted for $x = 0.1$. a_s decreases by more than 100 times as x decreases from 0.4 to 0.2, indicating the disappearance of spin glass order around a threshold concentration $x_{th} \approx 0.2$. Figure 3(b) shows the spin glass freezing temperature determined from these μSR measurements as a function of U concentration x.

The large nonmagnetic volume fraction in $Y_{0.8}U_{0.2}Pd_3$ is consistent with the existence of a nonmagnetic Γ_3 ground state, as identified by neutron scattering [16]. The weak magnetic order below $T_g \sim 1.0$ K seen in Fig.

2(a) might then be related to a possible small distribution of local U concentrations x. When x is very close to the threshold concentration x_{th}, the critical condition for spin glass order [Eq. (5)], as described below, may be fulfilled in regions of the sample where $x > x_{th}$.

The spin glass order in $Y_{0.6}U_{0.4}Pd_3$ and UPd_4 can be understood in the context of induced moments. For magnetic ions with a nonmagnetic ground state in the presence of a CEF, the mean field theory of Sherrington [17] gives a critical condition for cooperative spin glass order

$$\sqrt{z}J > \Delta_{CEF}/2\alpha_J^2, \quad (4)$$

where J is the exchange coupling constant of the Edwards-Anderson type Hamiltonian (standard deviation of randomly distributed J_{ij}), z is the coordination number of each magnetic ion, Δ_{CEF} is the energy separation between the CEF nonmagnetic ground state $|0\rangle$ and the first excited state $|1\rangle$, and $\alpha_J = \langle 0|J_z|1\rangle$. The induced moment picture has been used to explain spin glass behavior and neutron scattering results in PrP_y [18]. Using the magnetic moment per U ion $\mu \approx 1\mu_B$ [15] and $\Delta_{CEF} = 6$ meV [16] determined by neutron scattering, $\alpha_J = \langle \Gamma_3|J_z|\Gamma_5\rangle = 2$ and $z = 5$, we estimate the coupling constant J to be ~ 0.6 meV for UPd_4 [19], consistent with the ordering temperature $k_B T_g \approx 1.1$ meV. We see that the critical condition for spin glass order [Eq. (5)] holds for UPd_4. If we assume that the coupling constant J, Δ_{CEF}, and α_J are independent of x and the average coordination number $\langle z\rangle = 6x$, the critical condition for spin glass order would become $x > 0.3$. These calculations demonstrate that the observed crossover from nonmagnetic to spin glass ground states at $x_{th} \approx 0.2$ can be explained by the induced moment picture, using parameters consistent with the observed values of Δ_{CEF}, kT_g, and μ.

An alternative possible explanation is that the disappearance of spin glass freezing at $x_{th} \approx 0.2$ is determined by the competition between single-ion Kondo screening of the U^{4+} moments and intrinsic exchange interactions. However, this seems unlikely since a threshold concentration $x_{th} = 0.1$–0.2 is also observed for the related $La_{1-x}U_xPd_3$ system in which the Kondo effect is not observed [13].

In conclusion, we have demonstrated that UPd_4 and $Y_{0.6}U_{0.4}Pd_3$ exhibit spin glass order, while the predominant volume fraction remains nonmagnetic at $T \to 0$ in $Y_{0.8}U_{0.2}Pd_3$. The large nonmagnetic volume fraction in $Y_{0.8}U_{0.2}Pd_3$ is consistent with the existence of a nonmagnetic Γ_3 ground state. The muon spin relaxation rate becomes even smaller in $Y_{0.9}U_{0.1}Pd_3$, indicating disappearance of magnetic order with decreasing x. We have also proposed a picture that, out of possible competitions among the Kondo effect, RKKY interaction, and crystal field effects, it is the latter two factors which dominate the magnetic phase diagram of the system.

We thank P. Allenspach, D. L. Cox, and R. P. Guertin for stimulating discussions, and C. Ballard and K. Hoyle for technical assistance. Work at Columbia University is supported by NSF Grant No. DMR-89-13784 and the Packard Foundation (Y.J.U.). Work at UCSD is supported by U.S. NSF Grant No. DMR 91-07698 and U.S. DOE Grant No. DE-FG03-86ER-45230.

*Present address: Physics Department, Brookhaven National Laboratory, Upton, NY 11973.

[1] J. Kondo, Prog. Theor. Phys. **32**, 37 (1964).

[2] J. Kondo, in *Solid State Physics*, edited by F. Seitz and D. Turnbull (Academic, New York, 1969), Vol. 23, p. 183.

[3] W. Low, in *Paramagnetic Resonance in Solids*, Solid State Physics supplement 2, edited by F. Seitz and D. Turnbull (Academic, New York, 1960).

[4] N. B. Brandt and V. V. Moshchalkov, in *Advances in Physics*, edited by D. Sherrington (Taylor & Francis, London, 1984), p. 373.

[5] D. L. Cox, Phys. Rev. Lett. **59**, 1240 (1987).

[6] C. L. Seaman *et al.*, Phys. Rev. Lett. **67**, 2882 (1991).

[7] C. L. Seaman *et al.*, J. Alloys Compounds **181**, 327 (1992); C. L. Seaman, Ph.D. thesis, University of California at San Diego, 1992. The existence of vacancies is determined through a comparison of measured and theoretical crystal densities.

[8] Preliminary results of ZF-μSR measurements in these systems were published in W. D. Wu *et al.*, Physica (Amsterdam) **186-188B**, 344 (1993).

[9] A. Schenck, *Muon Spin Rotation Spectroscopy* (Adam Hilger, Bristol, 1985).

[10] R. S. Hayano *et al.*, Phys. Rev. B **20**, 850 (1979).

[11] Y. J. Uemura *et al.*, Phys. Rev. B **31**, 546 (1985).

[12] We have used the following probability function:

$$\rho(\Delta,a) \propto \frac{1}{d^2+(\Delta/a-1/\sqrt{2})^2}\frac{a}{\Delta^2}\exp\left(-\frac{a^2}{2\Delta^2}\right),$$

which gives a Gaussian field distribution if $d=0$ and a Lorentzian field distribution if $d=\infty$, to analyze the μSR asymmetry. Details will be published in a forthcoming paper.

[13] Details will be published in a forthcoming paper.

[14] To obtain good fitting, the parameter β is fixed to $\frac{1}{2}$ below $T \approx T_g$ in both $Y_{0.6}U_{0.4}Pd_3$ and UPd_4, while allowed to take a free value above T_g. We obtained $\beta \approx \frac{1}{2}$ around T_g. For nearly Gaussian local fields, $\beta = \frac{1}{2}$ is expected when there is a wide distribution of the fluctuation rate ν (and consequently the relaxation rate $1/T_1$). The observed tendency of β may then suggest increasingly non-Markovian fluctuations around and below T_g.

[15] A. Murasik *et al.*, Phys. Status Solidi (a) **28**, K107 (1975).

[16] H. A. Mook *et al.*, Physica (Amsterdam) **186-188B**, 341 (1993).

[17] D. Sherrington, J. Phys. C **12**, L929 (1979).

[18] H. Yoshizawa *et al.*, Phys. Rev. B **27**, 448 (1983); S. K. Hasanain *et al.*, Phys. Rev. B **24**, 5165 (1981).

[19] This value of J is obtained using Eqs. 9(b)–12 of Ref. [17] and values of $\mu \approx 1\mu_B$, $\Delta = 6$ meV, $\alpha_J = 2$, and $z = 5$. An alternative way, using Eq. 9(b) only, with the values of $T_g = 12.5$ K, Δ, α_J, and z leads to $J \approx 0.4$ meV. This small difference reflects the fact that Sherrington's model does not perfectly represent the real system.